Title

Volcanoes Erupt Stressed Quartz Crystals

Journal

Geophysical Research Letters, 46(15)

ISSN

0094-8276

Authors

Befus, KS

Manga, M

Stan, C

et al.

Publication Date

2019-08-16

DOI

10.1029/2019gl083619

Peer reviewed

Volcanoes Erupt Stressed Quartz Crystals

K. S. Befus[1], M. Manga[2], C. Stan[3], and N. Tamura[3]

[1] Department of Geosciences, Baylor University, Waco, TX, USA, [2] Department of Earth and Planetary Science, University of California, Berkeley, CA, USA, [3] Advanced Light Source, Lawrence Berkeley National Laboratory, Berkeley, CA, USA

Correspondence to: K. S. Befus, Kenneth_Befus@Baylor.edu

Abstract

Volcanic eruptions are energetic events driven by the imbalance of magmatic forces. The magnitudes of these forces remain poorly constrained because they operate in regions that are inaccessible, either underground or dangerous to approach. New techniques are needed to quantify the processes that drive eruptions and to probe magma storage conditions. Here we present X-ray microdiffraction measurements of volcanic stress imparted as lattice distortions to the crystal cargo of magma from Yellowstone and Long Valley eruptions. Elevated residual stresses between 100 and 300 MPa are preserved in erupted quartz. Multiple volcanic forces could be culpable for the deformation so we analyzed crystals from pyroclastic falls, pyroclastic density currents, and effusive lavas. Stresses are preserved in all quartz but cannot be attributed to differences in eruption style. Instead, lattice deformation likely preserves an in situ measurement of the deviatoric stresses required for the brittle failure of viscous, crystal-bearing glass during ascent.

Plain Language Summary

Because of inherent danger, volcano scientists have little direct understanding of the stresses active during volcanic eruptions. We propose that the crystal cargo carried by a volcanic eruption may preserve a record of those stresses. We used synchrotron X-ray microdiffraction to measure crystal deformation in quartz from explosive and effusive eruptions from Yellowstone and Long Valley calderas. All the crystals were strained by stresses ranging from 100 to 300 MPa. These values are large but are not related to eruption style. The stresses may have been caused by crystal-crystal impingements in the crystal-rich magma chambers. More likely, we propose that the residual stresses record those required for brittle failure of the crystal-bearing melt in the conduit during eruptive ascent.

1 Introduction

Magma experiences stresses throughout its lifetime, including from storage prior to eruption, during ascent in conduits, and finally upon fragmentation and transport above ground (Gonnermann & Manga, 2007; Green et al., 2006; Gudmundsson, 2006; Malfait et al., 2014; Patanè et al., 2003). Magma transport, eruption explosivity, and volcanic hazards are all influenced by those stresses (Cabrera et al., 2015; Gardner et al., 2018; Gonnermann &

Manga, 2003; Tuffen et al., 2003). The magnitude and relative importance of the magmatic stresses on these outcomes, however, have not been measured. Here we provide the first measure of stresses that are preserved as deviatoric elastic strains in quartz crystals erupted from volcanoes. These stresses may have been conveyed during explosive fragmentation, shear in flowing lavas, or arise from crystal-crystal force chains while magma was stored prior to eruption (Bergantz et al., 2017).

To identify the processes that produced the residual stresses, we measured crystal lattice deformation in quartz crystals from a suite of eruptions at Long Valley and Yellowstone supervolcanoes using synchrotron Laue X-ray microdiffraction (μXRD) at the Advanced Light Source, Lawrence Berkeley National Laboratory, USA (Chen et al., 2015; Kunz, Chen, et al., 2009; Tamura et al., 2009). Strained crystals produce diffraction patterns with spots that are stretched, smeared, or misplaced (Chen et al., 2012). Elastic strain may be preserved even after external stresses are removed if internal stress-induced defects (vacancies or impurities), disinclinations, or dislocations lock strains into the crystal's structure. The preserved strain is considered *residual stress* held by the crystal lattice (Withers & Bhadeshia, 2001). Deviatoric elastic strain is the dominant effect measured using Laue μXRD, which is quantified by measuring the angular difference between the measured diffraction spot positions and those predicted for an ideal, nonstrained quartz lattice (Kunz, Chen, et al., 2009). Residual stress is computed from Hooke's law using the elastic stiffness tensor of quartz. We find that all crystals from eruptions at Yellowstone and Long Valley calderas are strained and thus preserve a record of magmatic stresses through the deformation of the ideal crystal.

2 Materials and Methods

Samples of high silica rhyolite pumice and obsidian were collected from outcrops of explosive and effusive eruptions from the Long Valley and Yellowstone calderas, USA. The samples were gently crushed and then sieved. We handpicked a suite of 1- to 3-mm diameter quartz crystals from each unit (Table S1 in the supporting information). For all samples, crystals were prepared by mounting them in epoxy and grinding them to produce polished, flat cross sections of grain interiors.

We analyzed all quartz crystals using synchrotron X-ray microdiffraction (μXRD) at beamline 12.3.2 of the Advanced Light Source, Lawrence Berkeley National Laboratory, USA (Kunz, Tamura, et al., 2009; Stan & Tamura, 2018; Tamura et al., 2009). The synchrotron source produces a very bright, high flux X-ray beam ($\sim 10^{12}$ photons s^{-1}) over a wide, polychromatic energy range of 5–24 keV. The incident X-ray beam is focused on the sample via a system with Kirkpatrick-Baez mirrors and produces a stable spot size of ~1 μm^2. The sample is mounted on a mobile scanning stage driven by motors with submicron control in both orthogonal directions in the plane of the sample surface. Diffraction patterns were collected using a DECTRIS Pilatus 1M

detector. We produced 35 µXRD microstructural maps of individual quartz crystals, collected on 5 separate visits to the Advanced Light Source from 2016 to 2018. Individual mapping experiments lasted between 2 and 4 hr, depending on the area analyzed and step size. For reference, a typical experiment involved a ~300 by ~300 µm domain of a crystal using a ~1 μm^2 spot and a 4 µm step. Exposure time for each analysis was 1 s.

All measurements were performed in Laue diffraction mode, in which polychromatic X-rays impinge upon a stationary sample at a fixed angle, such that crystal lattice planes satisfy Bragg's law for specific wavelengths. Each set of lattice planes in the crystal diffracts the X-ray beam to produce a spot, and the positions of the spots are a function of the lattice spacing and symmetry of the crystal (Figure 1). The Laue diffraction patterns are automatically indexed using the X-Ray Microdiffraction Analysis Software (XMAS, Tamura, 2014), providing information on crystallographic orientation, deviatoric strain, crystal dislocations, and other defects. Strained crystals produce Laue diffraction patterns with spots that are stretched, smeared, or misplaced (Chen et al., 2012). Crystals may be strained by plastic or elastic deformation. Smeared spots in the diffraction pattern record dislocation density from plastic deformation (Chen et al., 2015). Domains within many of the quartz crystals preserve µXRD evidence for plastic deformation, but petrographic observations of the crystals never identify structures produced by plastic deformation, such as undulatory extinction, lamellae, or subgrain boundaries. Because we are unable to extract causal magmatic stresses we do not address plastic deformation here.

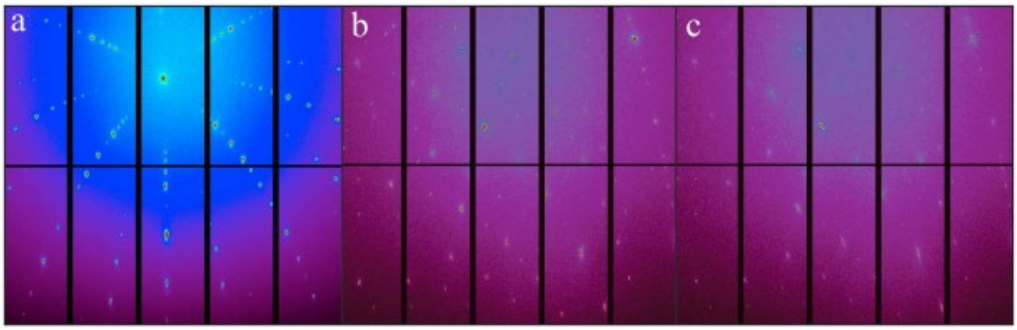

Figure 1. Laue µXRD patterns for (a) an undeformed quartz standard, (b) less deformed, and (c) more deformed domains of a single quartz crystal from the Tuff of Bluff Point, Yellowstone caldera. The positions of the spots reflect lattice spacing and crystal symmetry, which is why Figure 1a has different spot positions than Figures 1b and 1c. Plastic strain produces smeared spots, whereas elastic strain is a function of the differences between the measured positions and those predicted for an ideal, unstrained crystal.

In this study, we focus on deviatoric elastic strains. These can be considered the strains that are associated with the shear components of the strain tensor, after the isotropic strain is removed. Geobarometers are used to constrain the hydrostatic or lithostatic pressure that some parcel of rock or magma experienced. Those pressures are isotropic stresses and are not the stresses measured with Laue µXRD. Instead, we calculate deviatoric elastic stresses that cause nonorthogonal distortion to the crystal structure. Deviatoric elastic strains are determined by measuring the angular

differences between the Laue pattern spot positions and those predicted for an ideal, unstrained crystal (Chen et al., 2012; Kunz, Chen, et al., 2009). The uncertainty of a strain measurement is a function of the number of diffraction spots and the crystal lattice standard used in XMAS. Prior to our experiment, analyses of an unstrained synthetic hydrothermal quartz crystal suggest the instrumental uncertainty for quartz is 0.3×10^{-3} strain, which is at least an order of magnitude less than strains measured in the target, strained quartz crystals (supporting information Figure S1).

Elastic strains should relax when stresses are removed, but each quartz crystal from the Long Valley and Yellowstone calderas preserve elastic strains. This demonstrates that the lattice and lattice defects preserve internal residual stresses that retain elastic strain (Noyan & Cohen, 2013). Hexagonal β quartz is the thermodynamically stable polymorph of silica in the majority of rhyolitic, quartz-producing, magmatic systems. During cooling, β quartz spontaneously and reversibly undergoes a displacive transformation to trigonal α quartz (Heaney & Veblen, 1991). The change in symmetry produces a 0.86% change in volume such that α quartz is denser, but the strain occurs orthogonal to the axes and does not change axial angles. Laue diffraction μXRD only measures deviatoric elastic strain; thus, α-β transition strains are not expected to modify deviatoric strains caused by magmatic stresses (Carpenter et al., 1998).

We quantify the residual stress by employing Hooke's law, which relates stress to strain: $\sigma'_{ij} = c_{ijkl} * \varepsilon'_{kl}$ where σ'_{ij} is the deviatoric stress tensor, ε'_{kl} is the measured deviatoric strain tensor, and c_{ijkl} is the elastic stiffness tensor of the mineral. The elastic stiffness constants of β quartz are 120, 10, 35, 116, 40, and 50 GPa for the $c11$, $c12$, $c13$, $c33$, $c44$, and $c66$ orientations, respectively (Carpenter et al., 1998). XMAS uses these elastic stiffness constants and the measured strain in each sample to generate microstructural maps of the residual stress. We report residual stress as von Mises stress, which serves as a scalar measure of the magnitude of shear deformation prior to plastic yield. The reported residual stress for each sample represents the mean and 1σ standard deviation of the individual spot measurements, n, whose distributions produce the stress maps. Residual stress uncertainty is estimated to be ~30 MPa, which we calculated using the observed distribution of residual stress in the undeformed quartz standard. The standard was prepared as a thin section similar to unknowns; thus, sectioning, grinding, and polishing effects are minimal.

3 Results

We mapped two-dimensional domains of residual stresses preserved within crystal interiors at micron-scale spatial resolution (Figure 2 and supporting information Figures S2–S9 for all other crystals). Crystal domains from Yellowstone and Long Valley all preserve near-Gaussian probability distributions of residual stress with means between 90 and 220 MPa. The positively skewed tails in the distributions are produced by subdomains of

higher residual stress along curvilinear crystal defects and linear dislocation bands that account for 1 to 15% of the mapped areas. Here we restrict our analyses to the overall stress distributions preserved within the mapped domains, rather than providing a detailed analysis of the full range of microstructures (see Figures S2–S9). To isolate the contributing processes and environments that produced the deformation, we analyzed the residual stresses in quartz crystals from eruptions with a range of eruption styles, magnitudes, ages, and volumes (Table 1). Crystals from individual eruptions preserve similar residual stresses, marked with consistent means and standard deviations. Noticeable differences exist between crystals from separate eruptions, likely resulting from different preeruptive magmatic conditions or eruption dynamics.

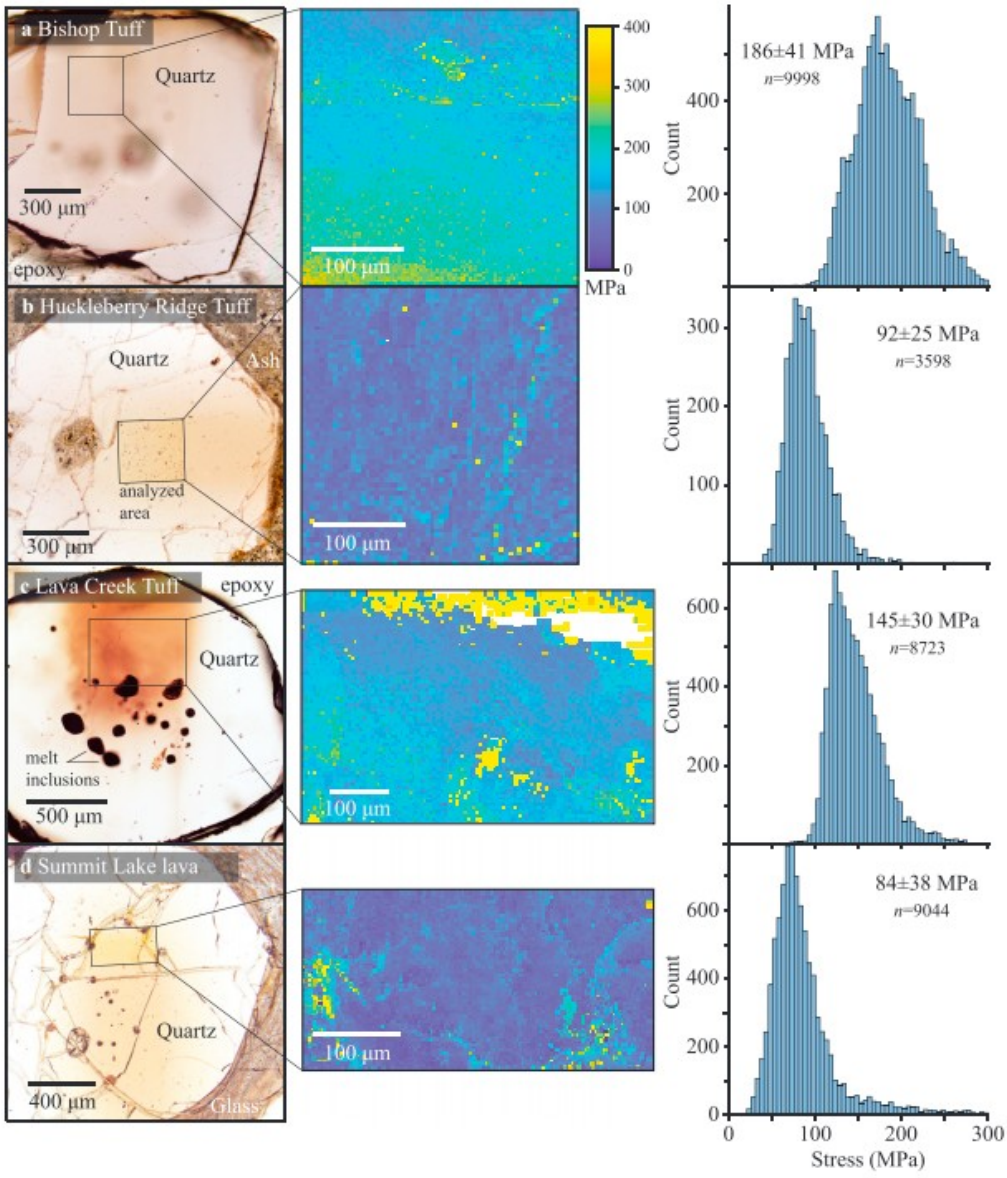

Figure 2. Quartz crystals preserve strain shown here in photomicrographs, 2D von Mises residual stress maps, and probability distributions of stress for representative samples from (a) Bishop Tuff, (b) Huckleberry Ridge Tuff, (c) Lava Creek Tuff, and (d) Summit Lake lava flow. The residual stress scale is the same for all maps and is shown in Figure 2a. Color and texture differences in the analyzed domains (Figures 2b–2d) are produced by beam damage to epoxy, not the quartz.

Table 1
Eruption Characteristics and Residual Stresses in Quartz

Caldera	Eruption unit	Eruption style	Age (ka)	Volume (km^3)	Stress (MPa)	n
Long Valley, USA	Bishop Tuff Fall	Explosive (Fall[a])	759 ± 4	650	210 ± 53	4 (16595)
	Bishop Tuff PDC	Explosive (PDC[a])			193 ± 37	2 (11018)
Yellowstone, USA	Huckleberry Ridge Tuff	Explosive (PDC)	2053 ± 6	2160	115 ± 45	5 (19696)
	Mesa Falls Tuff	Explosive (Fall)	1,292 ± 5	300	226 ± 71	4 (30058)
	Lava Creek Tuff	Explosive (PDC)	640 ± 2	1000	145 ± 47	4 (19420)
	Tuff of Bluff Point	Explosive (PDC)	173 ± 5	50	112 ± 34	6 (21407)
	Summit Lake Lava	Effusive (near vent)	124 ± 10	37	113 ± 41	5 (19442)
	Summit Lake Lava	Effusive (distal)			126 ± 66	5 (28439)

Note. Data for Long Valley (Hildreth, 2004; Sarna-Wojcicki et al., 2000; Wilson & Hildreth, 1997). Data for Yellowstone (Christiansen, 2001; Christiansen et al., 2007). *n* is the number of analyzed crystals with the combined number of individual spot μXRD analyses in parentheses. μXRD = synchrotron X-ray microdiffraction.
[a]Fall is emplacement by settling in pyroclastic fall, whereas PDC indicates emplacement via pyroclastic density current.

3.1 No Strain From Pyroclastic Surface Processes

The influence of pyroclastic transport processes on crystal strain was evaluated using the Bishop Tuff. The Bishop Tuff contains interbedded pyroclastic fall and pyroclastic density current deposits generated contemporaneously by the supereruption from Long Valley caldera at ~760 ka (Hildreth, 2004). Pyroclastic density currents form when the eruption column fails to ingest sufficient atmosphere to buoyantly rise, causing the eruption column to collapse into a turbulent density current of volcanic gas, ash, pumice, and crystals. Conversely, pyroclastic fall deposits are produced by the comparatively gentle gravitational settling of pumice, ash, and crystals from the umbrella region of a fully buoyant eruption column. Importantly, the magmatic and fragmentation processes that lead to pyroclastic fall and pyroclastic density currents are identical. Thus, crystal deformation prior to eruption for both processes should be the same. Bishop Tuff quartz crystals preserve the same amount of residual stress (~200 MPa) in both the pyroclastic fall and pyroclastic density currents, indicating that pyroclastic processes have no detectable effect on lattice strain. Preserved stresses in the Bishop Tuff quartz instead record subsurface processes.

3.2 No Strain From Lava Transport

Elastic strain in quartz crystals from near-vent and distal portions of the Summit Lake rhyolitic obsidian lava at Yellowstone caldera was measured to isolate the contribution of viscous shear stress on quartz deformation during transport in a lava flow. The near-vent and distal samples traveled <200 m and ~9 km from the vent, respectively. Near-vent quartz crystals preserve stresses of 113 ± 41 MPa, with some variability between and within samples. The distal crystals preserve stresses of 126 ± 66 MPa, indistinguishable from the near-vent crystals. Shear during lava emplacement did not significantly modify the residual stresses, again suggesting that crystal deformation must record subsurface magmatic processes.

3.3 Similar Strain From Different Eruption Styles

We assess the contribution of fragmentation culminating in explosive eruption by comparing preserved stresses in quartz from the explosive Tuff

of Bluff Point and the near-vent Summit Lake lava. The Tuff of Bluff Point and Summit Lake lava are age-equivalent, high silica rhyolites that are magmatically consanguineous (Befus & Gardner, 2016; Christiansen, 2001). Efficient gas loss during ascent led to effusion of the Summit Lake lava. Conversely, the Tuff of Bluff Point magma was unable to degas during ascent and instead erupted in a powerful explosive eruption that produced a large caldera. Crystals from the explosive Tuff of Bluff Point have low residual stresses of 112 ± 34 MPa, similar to the Summit Lake lava, indicating that different fragmentation and eruption processes within the conduit did not cause resolvable differences in deviatoric elastic strains.

4 Discussion

Uniformly, quartz crystals from eruptions at Long Valley and Yellowstone preserve elevated residual stress. Several magmatic environments could impart such stresses. Initially, crystal-containing magmas were stored in chambers where crystal-crystal impingement may exert compressive stresses (Bachmann & Bergantz, 2004; Cooper & Kent, 2014). Eruptions only begin after the crystal mush is mobilized, likely by a thermal event (Burgisser & Bergantz, 2011; Huber et al., 2011; Mahood, 1990). After the eruption begins, magma ascending a conduit experiences viscous shear against conduit walls, potentially straining the lattices of the crystal cargo (Hale & Mühlhaus, 2007; Polacci et al., 2001). Magma viscosity increases substantially during ascent as it degasses (Giordano et al., 2008). If the magma becomes too viscous then it can fragment leading to an explosive volcanic eruption (Caricchi et al., 2007; Papale, 1999). Rarefaction waves produced during fragmentation would induce tensile stress in crystals (Best & Christiansen, 1997). Postfragmentation, high-velocity crystal collisions in the conduit or during deposition from pyroclastic density currents, may produce compressive deformation in the crystals (van Zalinge et al., 2018). Finally, magmas may effuse to form lava flows. Although nonexplosive, crystals in lavas may record the accumulation of significant viscous shear produced during emplacement (Kendrick et al., 2017). During an eruption, many processes may deform crystals via tension, compression, or shear stresses.

The key observation from our measurements is that the residual stresses from effusive and explosive eruptions, large and small eruptions, and proximal and distal samples are similar. This implies that stresses arise where magma is stored in reservoirs or during ascent in conduits.

4.1 Is Strain Imparted in the Magma Reservoir?

Our analyses of samples with distinct histories indicate that quartz lattice deformation may be the vestige of forces applied to crystals in the magma chamber environment, rather than from surface or conduit processes (Figure 3). This lattice strain does not originate from melt inclusions because we do not see a decay of strain away from melt inclusions (Figure 2).

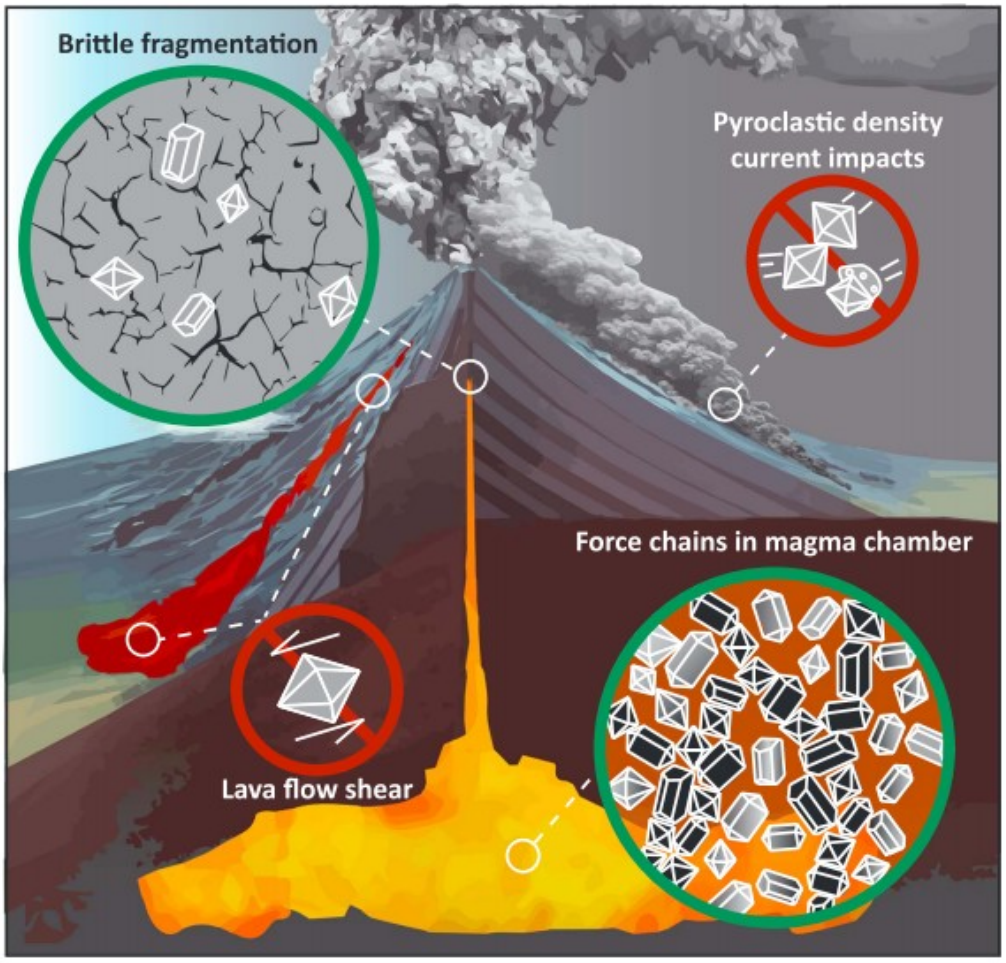

Figure 3. Potential causes of residual stress in volcanic crystals. Stresses maybe related to brittle fragmentation during ascent, or they are generated in the magma chamber where force chains, depicted in black, redistribute lithostatic stress. Volcano schematic after USGS circular.

Strained quartz crystals at Long Valley and Yellowstone may provide the mineral physics evidence to support the widespread notion that the magmas originated from crystal mushes that in turn were the source of erupted crystal cargo. Compelling lines of petrologic and seismic evidence suggest that most silicic magmas may reside in the crust as bodies of liquid-poor crystal mush for much of their lifetime (Bachmann & Bergantz, 2004). The crystal mush is conceived as a porous network of touching crystals. Crystal-crystal contacts support the crystal mush (Bergantz et al., 2017). Short duration thermal events precede volcanic eruptions, which defrost and mobilize the crystal network and allow crystal-bearing magmas to erupt (Burgisser & Bergantz, 2011; Cooper & Kent, 2014; Mahood, 1990).

In magma mushes, as crystals impinge upon each other they create force chains between particles (e.g., Bergantz et al., 2017). The force chain model for the generation and preservation of residual stresses in quartz makes two predictions that are not obviously consistent with our measurements. First,

the spatial distribution of stresses within crystals differs from that expected in a mush. Hertzian contacts between particles should produce gradients in stress with magnitudes that decay away from contacts (Johnson, 1985). About a third of our stress maps preserve gradients across subdomains within the crystals, but these are not clearly related to particle contacts. Other variations are found along curvilinear trends within the crystals instead of domains near the margins. Second, we do not see a range of mean stresses similar to that expected for a mush. In a packed granular material, the force chains between particles create a distribution of forces on particles that decays approximately exponentially above the mean and is closer to uniform below the mean (e.g., Radjai et al., 1999). The details of the distribution are sensitive to the history of deformation, the types of applied stresses, the degree of crystal packing, and other types of heterogeneity (e.g., Bergantz et al., 2017; Majumdar & Behringer, 2005). We should thus expect to find crystals with a range of stresses, from negligible to much greater than the mean—this variability arises because the stresses are supported by some crystals in force chains whereas others are in stress shadows. We are not able to measure the large number of crystals needed to determine the distribution of mean residual stresses that could be quantitatively compared with those from experimental studies or numerical simulations. However, all quartz from a specific eruption have similar residual stresses and we do not see crystals with the low stresses expected from the predicted force chain distributions. One way to remove a wide distribution of stress would be for force chains to repeatedly break down and reform by the stirring or remobilization of magma bodies such that all crystals spend some time in force chains. Indeed, force chains are expected to be ephemeral. If so, the stresses are preserved rather than relax when crystals leave force chains.

Despite these two apparent weaknesses, the force chain model remains appealing because, if correct, it might provide a measureable mechanical window into magma mushes. The mean stress is equal to the confining pressure (e.g., Sun et al., 2015). The mean residual stress we measured is, in fact, similar to the storage pressure of the magmas. The magnitudes of preserved residual stresses in quartz from the Bishop Tuff are indistinguishable from preeruptive petrologic estimates of storage pressures that range from 170 to 220 MPa based on melt inclusions and petrologic geobarometers (Wallace et al., 1999). Residual stresses in Yellowstone quartz range from 100 to 250 MPa. Such values align with petrologically inferred storage depths for past eruptions and with geophysical imaging of Yellowstone's modern, but volcanically dormant, magmatic system (Befus & Gardner, 2016; Farrell et al., 2014; Myers et al., 2016).

Given the two shortcomings we identified, we thus provide an alternative, conduit-level explanation for the preservation of residual stresses in quartz crystals from supervolcanoes.

4.2 Shear stresses at the fragmentation threshold

Preserved residual stresses in quartz crystals are very similar, ranging only by a factor of ~2, irrespective of volcano geography, eruption size, or eruptive mechanism. Such similarity suggests that a shared process deformed these crystals during ascent. We propose that the deviatoric elastic strain preserved in the quartz crystals may be an in situ measure of the fragmentation threshold in the conduit. Indeed, our residual stress measurements of 90 to 220 MPa correspond to experimental limits for the shear stresses associated with failure of rhyolite, which have been shown to be ~100 MPa (Cordonnier et al., 2012; Wadsworth et al., 2018). Prior to fragmentation, viscous deformation in the conduit produces similar stresses in both the melt and crystals. When those stresses become large enough the melt fragments and the strained crystals preserve a record of the stress. Both explosive and effusive fragmentation events could thus produce the same strain because it is related to the shear stresses required for the brittle failure of viscous, crystal-bearing glass. If true, then pyroclastic explosions may fragment once and directly record associated shear stresses in the crystal cargo. Textures of natural and experimental samples suggest that effusive silicic magmas may also fragment but subsequently reweld in the conduit (Gardner et al., 2018; Tuffen et al., 2003). It remains uncertain if the process occurs once or countless times (Gonnermann & Manga, 2003). Residual stresses in quartz crystals from effusive eruptions are indistinguishable from explosive eruptions, supporting the inference that these magmas also fragmented during ascent.

Relative timing constraints may provide additional clues that deformation was a conduit process. Quartz crystals from Long Valley and Yellowstone are marked by pronounced growth bands visible in CL (Girard & Stix, 2010; Loewen & Bindeman, 2015). Quartz crystals from the Bishop Tuff have bright, Ti-rich rims that may have grown in the days and months preceding the eruption (Gualda & Sutton, 2016). However, μXRD maps spanning core to rim positions in Bishop Tuff quartz crystals show no differences in residual stress. Similarly, residual stresses in Yellowstone quartz do not correlate with growth banding. Together, these observations support the theory that deviatoric strains were imparted after crystal growth, possibly by shear stresses leading up to fragmentation in the conduit.

5 Final Thoughts

Recent advances in microanalytical capabilities and interpretation allow geochemical measurements within crystals to be used as *clocks in rocks*, providing new insights into timescales for magma storage, mobilization, mixing, and ascent (National Academies of Sciences, Engineering, and Medicine, 2017). Microscale measurements of residual stresses offer new, complementary insights into the mechanical state and evolution of magmas prior to, or during, an eruption. Here we show that for all erupted magmas, whether explosive or effusive, the residual stresses are similar and hence originate prior to erupting on the surface. We propose that the strains are an in situ measure of the fragmentation threshold in the conduit, which

previously has only been estimated with lab experiments. Further experimental studies to quantify how crystals are deformed and stresses relax, combined with additional analytical techniques (e.g., electron backscatter diffraction and transmission electron microscopy; Dresen et al., 1997; Wallis et al., 2017) and samples from other volcanic systems, may help us more reliably distinguish stresses from fragmentation and those inherited from magma bodies.

Acknowledgments

We thank T. C. Leonhardi for preparing samples, performing analyses, and contributing in discussions about the interpretations. We also thank George Bergantz, Fabian Wadsworth, and anonymous reviewers for insightful discussion. Samples from Yellowstone were collected under National Park Service research permits YELL-07072 and YELL-05678. This research was supported by NSF EAR 1724429, awarded to K. B. and M. M. with support from NSF 1521855 and Larsen fund for field sampling. This research used beamline 12.3.2 of the Advanced Light Source with all beamline data archived at the National Energy Research Scientific Computer Center, which are both DOE Office of Science User Facilities under contract DE-AC02-05CH11231. Data are available in the main text and in the supporting information.

References

Bachmann, O., & Bergantz, G. W. (2004). On the origin of crystal-poor rhyolites: Extracted from batholithic crystal mushes. *Journal of Petrology*, 45(8), 1565– 1582. https://doi.org/10.1093/petrology/egh019

Befus, K. S., & Gardner, J. E. (2016). Magma storage and evolution of the most recent effusive and explosive eruptions from Yellowstone caldera. *Contributions to Mineralogy and Petrology*, 171(4), 30. https://doi.org/10.1007/s00410-016-1244-x

Bergantz, G. W., Schleicher, J. M., & Burgisser, A. (2017). On the kinematics and dynamics of crystal-rich systems. *Journal of Geophysical Research: Solid Earth*, 122, 6131– 6159. https://doi.org/10.1002/2017JB014218

Best, M. G., & Christiansen, E. H. (1997). Origin of broken phenocrysts in ash-flow tuffs. *Geological Society of America Bulletin*, 109(1), 63– 73. https://doi.org/10.1130/0016-7606(1997)109<0063:OOBPIA>2.3.CO;2

Burgisser, A., & Bergantz, G. W. (2011). A rapid mechanism to remobilize and homogenize highly crystalline magma bodies. *Nature*, 471(7337), 212– 215. https://doi.org/10.1038/nature09799

Cabrera, A., Weinberg, R. F., & Wright, H. M. N. (2015). Magma fracturing and degassing associated with obsidian formation: The explosive-effusive transition. *Journal of Volcanology and Geothermal Research*, 298, 71– 84. https://doi.org/10.1016/j.jvolgeores.2014.12.014

Caricchi, L., Burlini, L., Ulmer, P., Gerya, T., Vassalli, M., & Papale, P. (2007). Non-Newtonian rheology of crystal-bearing magmas and implications for magma ascent dynamics. *Earth and Planetary Science Letters*, 264(3–4), 402– 419. https://doi.org/10.1016/j.epsl.2007.09.032

Carpenter, M. A., Salje, E. K., Graeme-Barber, A., Wruck, B., Dove, M. T., & Knight, K. S. (1998). Calibration of excess thermodynamic properties and elastic constant variations associated with the <- > phase transition in quartz. *American Mineralogist*, 83(1-2), 2– 22. https://doi.org/10.2138/am-1998-1-201

Chen, K., Dejoie, C., & Wenk, H.-R. (2012). Unambiguous indexing of trigonal crystals from white-beam Laue diffraction patterns: Application to Dauphiné twinning and lattice stress mapping in deformed quartz. *Journal of Applied Crystallography*, 45(5), 982– 989. https://doi.org/10.1107/S0021889812031287

Chen, K., Kunz, M., Tamura, N., & Wenk, H.-R. (2015). Residual stress preserved in quartz from the San Andreas Fault Observatory at depth. *Geology*, 43(3), 219– 222. https://doi.org/10.1130/G36443.1

Christiansen, R. L. (2001). The Quaternary and Pliocene Yellowstone plateau volcanic field of Wyoming, Idaho, and Montana, USGS Numbered Series Rep. 729-G.

Christiansen, R. L., Lowenstern, J. B., Smith, R. B., Heasler, H., Morgan, L. A., Nathenson, M., Mastin, L. G., Muffler, L. J. P., & Robinson, J. E. (2007). Preliminary assessment of volcanic and hydrothermal hazards in Yellowstone National Park and vicinity, USGS Numbered Series Rep. 2007-1071.

Cooper, K. M., & Kent, A. J. (2014). Rapid remobilization of magmatic crystals kept in cold storage. *Nature*, 506(7489), 480– 483. https://doi.org/10.1038/nature12991

Cordonnier, B., Caricchi, L., Pistone, M., Castro, J., Hess, K. U., Gottschaller, S., Manga, M., Dingwell, D. B., & Burlini, L. (2012). The viscous-brittle transition of crystal-bearing silicic melt: Direct observation of magma rupture and healing. *Geology*, 40(7), 611– 614. https://doi.org/10.1130/G3914.1

Dresen, G., Duyster, J., Stöckhert, B., Wirth, R., & Zulauf, G. (1997). Quartz dislocation microstructure between 7000 m and 9100 m depth from the Continental Deep Drilling Program KTB. *Journal of Geophysical Research*, 102(B8), 18,443– 18,452. https://doi.org/10.1029/96JB03394

Farrell, J., Smith, R. B., Husen, S., & Diehl, T. (2014). Tomography from 26 years of seismicity revealing that the spatial extent of the Yellowstone crustal magma reservoir extends well beyond the Yellowstone caldera. *Geophysical Research Letters*, 41, 3068– 3073. https://doi.org/10.1002/2014GL059588

Gardner, J. E., Wadsworth, F. B., Llewellin, E. W., Watkins, J. M., & Coumans, J. P. (2018). Experimental sintering of ash at conduit conditions and

implications for the longevity of tuffisites. *Bulletin of Volcanology*, 80(3), 23. https://doi.org/10.1007/s00445-018-1202-8

Giordano, D., Russell, J. K., & Dingwell, D. B. (2008). Viscosity of magmatic liquids: A model. *Earth and Planetary Science Letters*, 271(1-4), 123– 134. https://doi.org/10.1016/j.epsl.2008.03.038

Girard, G., & Stix, J. (2010). Rapid extraction of discrete magma batches from a large differentiating magma chamber: The Central Plateau Member rhyolites, Yellowstone Caldera, Wyoming. *Contributions to Mineralogy and Petrology*, 160(3), 441– 465. https://doi.org/10.1007/s00410-009-0487-1

Gonnermann, H. M., & Manga, M. (2003). Explosive volcanism may not be an inevitable consequence of magma fragmentation. *Nature*, 426(6965), 432– 435. https://doi.org/10.1038/nature02138

Gonnermann, H. M., & Manga, M. (2007). The fluid mechanics inside a volcano. *Annual Review of Fluid Mechanics*, 39(1), 321– 356. https://doi.org/10.1146/annurev.fluid.39.050905.110207

Green, D., Neuberg, J., & Cayol, V. (2006). Shear stress along the conduit wall as a plausible source of tilt at Soufrière Hills volcano, Montserrat. *Geophysical Research Letters*, 33, L10306. https://doi.org/10.1029/2006GL025890

Gualda, G. A., & Sutton, S. R. (2016). The year leading to a supereruption. *PloS one*, 11(7), e0159200. https://doi.org/10.1371/journal.pone.0159200

Gudmundsson, A. (2006). How local stresses control magma-chamber ruptures, dyke injections, and eruptions in composite volcanoes. *Earth-Science Reviews*, 79(1-2), 1– 31. https://doi.org/10.1016/j.earscirev.2006.06.006

Hale, A. J., & Mühlhaus, H.-B. (2007). Modelling shear bands in a volcanic conduit: Implications for over-pressures and extrusion-rates. *Earth and Planetary Science Letters*, 263(1-2), 74– 87. https://doi.org/10.1016/j.epsl.2007.08.026

Heaney, P. J., & Veblen, D. R. (1991). Observations of the alpha-beta phase transition in quartz: A review of imaging and diffraction studies and some new results. *American mineralogist*, 76(5-6), 1018– 1032.

Hildreth, W. (2004). Volcanological perspectives on Long Valley, Mammoth Mountain, and Mono Craters: Several contiguous but discrete systems. *Journal of Volcanology and Geothermal Research*, 136(3-4), 169– 198. https://doi.org/10.1016/j.jvolgeores.2004.05.019

Huber, C., Bachmann, O., & Dufek, J. (2011). Thermo-mechanical reactivation of locked crystal mushes: Melting-induced internal fracturing and assimilation processes in magmas. *Earth and Planetary Science Letters*, 304(3-4), 443– 454. https://doi.org/10.1016/j.epsl.2011.02.022

Johnson, K. L. (1985). *Contact mechanics*. Cambridge: Cambridge University Press. https://doi.org/10.1017/CBO9781139171731

Kendrick, J., Lavallée, Y., Mariani, E., Dingwell, D., Wheeler, J., & Varley, N. (2017). Crystal plasticity as an indicator of the viscous-brittle transition in magmas. *Nature communications*, 8(1), 1926. https://doi.org/10.1038/s41467-017-01931-4

Kunz, M., Chen, K., Tamura, N., & Wenk, H.-R. (2009). Evidence for residual elastic strain in deformed natural quartz. *American Mineralogist*, 94(7), 1059– 1062. https://doi.org/10.2138/am.2009.3216

Kunz, M., Tamura, N., Chen, K., MacDowell, A. A., Celestre, R. S., Church, M. M., Fakra, S., Domning, E. E., Glossinger, J. M., Kirschman, J. L., Morrison, G. Y., Plate, D. W., Smith, B. V., Warwick, T., Yashchuk, V. V., Padmore, H. A., & Ustundag, E. (2009). A dedicated superbend X-ray microdiffraction beamline for materials, geo-, and environmental sciences at the advanced light source. *Review of Scientific Instruments*, 80(3), 035108. https://doi.org/10.1063/1.3096295

Loewen, M. W., & Bindeman, I. N. (2015). Oxygen isotope and trace element evidence for three-stage petrogenesis of the youngest episode (260–79 ka) of Yellowstone rhyolitic volcanism. *Contributions to Mineralogy and Petrology*, 170(4), 1– 25.

Mahood, G. (1990). Second reply to comment of RSJ Sparks, HE Huppert and CJN Wilson on “Evidence for long residence times of rhyolitic magma in the Long Valley magmatic system: The isotopic record in the precaldera lavas of Glass Mountain”. *Earth and Planetary Science Letters*, 99(4), 395– 399. https://doi.org/10.1016/0012-821X(90)90145-N

Majumdar, T. S., & Behringer, R. P. (2005). Contact force measurements and stress-induced anisotropy in granular materials. *Nature*, 435(7045), 1079–1082. https://doi.org/10.1038/nature03805

Malfait, W. J., Seifert, R., Petitgirard, S., Perrillat, J.-P., Mezouar, M., Ota, T., Nakamura, E., Lerch, P., & Sanchez-Valle, C. (2014). Supervolcano eruptions driven by melt buoyancy in large silicic magma chambers. *Nature Geoscience*, 7(2), 122– 125. https://doi.org/10.1038/ngeo2042

Myers, M. L., Wallace, P. J., Wilson, C. J., Morter, B. K., & Swallow, E. J. (2016). Prolonged ascent and episodic venting of discrete magma batches at the onset of the Huckleberry Ridge supereruption, Yellowstone. *Earth and Planetary Science Letters*, 451, 285– 297. https://doi.org/10.1016/j.epsl.2016.07.023

National Academies of Sciences, Engineering, and Medicine (2017). *Volcanic eruptions and their repose, unrest, precursors, and timing*. Washington, DC: National Academies Press. https://doi.org/10.17226/24650

Noyan, I. C., & Cohen, J. B. (2013). *Residual stress: Measurement by diffraction and interpretation*. New York: Springer-Verlag.

Papale, P. (1999). Strain-induced magma fragmentation in explosive eruptions. *Nature*, 397(6718), 425– 428. https://doi.org/10.1038/17109

Patanè, D., De Gori, P., Chiarabba, C., & Bonaccorso, A. (2003). Magma ascent and the pressurization of Mount Etna's volcanic system. *Science*, 299(5615), 2061– 2063. https://doi.org/10.1126/science.1080653

Polacci, M., Papale, P., & Rosi, M. (2001). Textural heterogeneities in pumices from the climactic eruption of Mount Pinatubo, 15 June 1991, and implications for magma ascent dynamics. *Bulletin of Volcanology*, 63(2-3), 83– 97. https://doi.org/10.1007/s004450000123

Radjai, F., Roux, S., & Moreau, J. J. (1999). Contact forces in a granular packing. *Chaos*, 9(3), 544– 550. https://doi.org/10.1063/1.166428

Sarna-Wojcicki, A. M., Pringle, M. S., & Wijbrans, J. (2000). New 40Ar/39Ar age of the Bishop Tuff from multiple sites and sediment rate calibration for the Matuyama-Brunhes boundary. *Journal of Geophysical Research*, 105(B9), 21,431– 21,443. https://doi.org/10.1029/2000JB900901

Stan, C., & Tamura, N. (2018). Synchrotron X-ray microdiffraction and fluorescence imaging of mineral and rock samples. *Journal of Visualized Experiments*, 136, e57874.

Sun, Q., Jin, F., Wang, G., Song, S., & Zhang, G. (2015). On granular elasticity. *Scientific reports*, 5(1), 9652. https://doi.org/10.1038/srep09652

Tamura, N. (2014), XMAS: A versatile tool for analyzing synchrotron X-ray microdiffraction data, strain and dislocation gradients from diffraction. Spatially Resolved Local Structure and Defects, 125-155.

Tamura, N., Kunz, M., Chen, K., Celestre, R. S., MacDowell, A. A., & Warwick, T. (2009). A superbend X-ray microdiffraction beamline at the advanced light source. *Materials Science and Engineering: A*, 524(1–2), 28– 32. https://doi.org/10.1016/j.msea.2009.03.062

Tuffen, H., Dingwell, D. B., & Pinkerton, H. (2003). Repeated fracture and healing of silicic magma generate flow banding and earthquakes? *Geology*, 31(12), 1089. https://doi.org/10.1130/g19777.1

van Zalinge, M., Cashman, K., & Sparks, R. (2018). Causes of fragmented crystals in ignimbrites: A case study of the Cardones ignimbrite, Northern Chile. *Bulletin of Volcanology*, 80(3), 22. https://doi.org/10.1007/s00445-018-1196-2

Wadsworth, F. B., Witcher, T., Vossen, C. E., Hess, K.-U., Unwin, H. E., Scheu, B., Castro, J. M., & Dingwell, D. B. (2018). Combined effusive-explosive silicic volcanism straddles the multiphase viscous-to-brittle transition. *Nature communications*, 9(1), 4696. https://doi.org/10.1038/s41467-018-07187-w

Wallace, P. J., Anderson, A. T., & Davis, A. M. (1999). Gradients in H_2O, CO_2, and exsolved gas in a large-volume silicic magma system: Interpreting the record preserved in melt inclusions from the Bishop Tuff. *Journal of*

Geophysical Research, 104(B9), 20,097– 20,122. https://doi.org/10.1029/1999JB900207

Wallis, D., Hansen, L. N., Britton, T. B., & Wilkinson, A. J. (2017). Dislocation interactions in olivine revealed by HR-EBSD. *Journal of Geophysical Research: Solid Earth*, 122, 7659– 7678. https://doi.org/10.1002/2017JB014513

Wilson, C. J., & Hildreth, W. (1997). The Bishop Tuff: New insights from eruptive stratigraphy. *The Journal of Geology*, 105(4), 407– 440. https://doi.org/10.1086/515937

Withers, P. J., & Bhadeshia, H. (2001). Residual stress. Part 1—Measurement techniques. *Materials science and Technology*, 17(4), 355– 365. https://doi.org/10.1179/026708301101509980